SOURCE ANALYSIS AND CELLULAR INTERROGATION USING THE ELECTROENCEPHALOGRAM

Lauren Berryman (Electrical Engineering), University of Pennsylvania
NSF Summer Undergraduate Fellowship in Sensor Technologies
Advisors: Dr. Nader Engheta, Dr. Edward N. Pugh
Collaborators: Claire Daniele, Lauren Daniele

ABSTRACT

This paper describes the electroencephalographic detection and analysis of scalp potentials utilizing fMRI brain volume data to design stimuli that activate specific visual areas and pathways. Our dual purpose was to reevaluate current scientific models and to investigate the origin of neural activity in response to a specified stimulus. Through data collection and analysis, we tested the widely used three-shell conductivity model of the head. We concluded that this model is inappropriate for source analysis due to inherent model flaws and the disagreement of our experimental observations with model predictions. We approached the problem of dipole current source analysis by first pinpointing the source location within the visual cortex using collected metabolic fMRI data. Then, with our stimulus designed to activate that identified area of the cortex, we recorded electromagnetic scalp distribution patterns. By examining the collected sensory evoked potentials with Fourier analysis, we found frequency components present in the scalp recording at twice the stimulus flicker frequency. By tracing frequency response patterns and identifying corresponding contrast response parameters, we were able to show that for our stimulus, the magnocellular pathway was dominant in the flow of visual information from retina to cortex.

1. INTRODUCTION

The flow of visual information from the retina to the visual cortex follows a complex pathway created by the interconnections of a large number of neurons. In order to understand the general principles governing the transformation of sensory information in the brain, we must identify these cellular pathways and pinpoint active cells. Detection and analysis of brain activity patterns is the first step in the classification of complex cellular pathways. By stimulating specific areas of the visual cortex in the brain, we can trace the origins of neural activity by distinguishing patterns of brain activity that corresponds to the action of specific types of cells.

The response of cortical neurons begins with phototransduction and information processing in the retina. When light rays are reflected by an object, they enter the eye

and pass through the lens, which projects an inverted image onto the retina. Rod and cone cells in the retina send signals into the brain to the visual cortex. Neurons are responsible for the flow of information along this pathway and their activity in response to a visual stimulus can be detected at the surface of the scalp. The characteristics of this measurable scalp potential provide insight into the cellular pathways at work and the cells responsible.

Neural activity is detected and recorded with the electroencephalograph, or EEG. The EEG records the fluctuations of electrical activity through electrodes situated over the frontal, parietal, occipital, and temporal lobes. Each electrode detects the sensory-evoked potentials that reflect the cortical processing of the physical attributes of the stimulus. After EEG recording completion and subsequent separation of frequency components, the study of the signal's characteristics yields information about the activated visual pathways and cortical cells.

2. SCALP POTENTIAL AND CURRENT FLOW

2.1 Origin of Scalp Potential

Scalp potentials recorded by the EEG are generated in the cerebral cortex by pyramidal cells, a class of nerve cells. Pyramidal cells contribute more to the EEG than the second class of nerve cells, nonpyramidal cells, due to cellular orientation. Pyramidal cells are oriented parallel to one another and their dendrites are perpendicular to the surface of the cortex, allowing for minimal signal attenuation.

The apical dendrites of pyramidal cells are responsible for the generation of action potentials that amplify synaptic currents. Although action potentials are the largest signal generated by neurons, they actually contribute little to surface potentials. The main source of scalp potential recorded by the EEG results from extracellular current flow associated with summated synaptic potentials in the activated pyramidal cells. These synaptic potentials are slower than action potentials, which allows more time for signal summation [6].

In addition to dendritic projections, the axons of pyramidal cells also extend to other areas of the brain and spinal cord. Cellular projections that lie in a plane parallel to cortical layers play the most significant role in the generation of collective electrical activity. By facilitating the flow of synaptic currents through extracellular space, the axons are directly responsible for the measurable activity of cortical neurons.

Ionic current flow generated by the synchronous nerve cells through extracellular space can be described the theory of volume conduction. For a single pyramidal cell, potential is produced when a current flows across the resistance of the cell membrane. Current flows inward through the synaptic membrane and outward along the extrasynaptic membrane. This inward and outward current flow creates a current sink on the negative side of the extracellular potential and a source at the site of outward current so that the cells acts like a dipole (Figure 1).

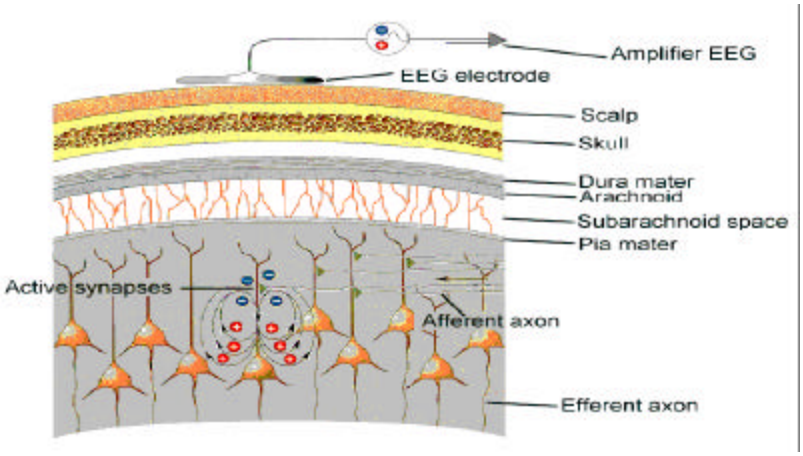

Figure 1: Pyramidal cells act as dipoles in the volume conductor of the head [2].

2.2 Measurement Of Scalp Potential

An electrode placed on the scalp records the summed signal from many cells. Depending on the orientation of the combined dipoles, the potential recorded at the scalp is either positive or negative. The recorded signal comes principally from neurons near the tip of the electrode and only to a small extent from more distant neurons. As the electrode is moved from the source of activity, the signal decreases by the square root of the distance. This rapid drop in potential combined with the large resistance of the scalp, skull and cerebrospinal fluid surrounding the brain results in a measured scalp potential that is very small. The frequencies of the potentials recorded from the surface of the scalp vary from 1 to 30 Hz, with amplitudes ranging from 20 to 100μV [6].

Analysis of the frequency components of the EEG is based on principles developed by mathematician Jean Baptiste Fourier. Fourier analysis expands the recorded signal voltage function into a series of sine wave harmonics. Electronic filtering methods used in combination with Fourier algorithms aid in analysis of the signal by separating frequency components (Figure 2).

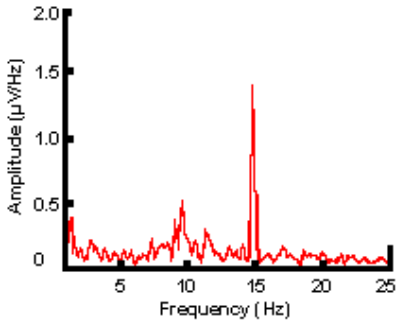

Figure 2: Frequency component at 15 Hz resulting from Fourier analysis of recorded scalp potential.

Source analysis using the EEG is an effective method because it records the voltage changes caused by neuronal currents. This is a more precise method of brain activity than other metabolic methods, such as the fMRI. While the fMRI measures gradual variations in blood flow and is useful for obtaining three-dimensional brain volume visualizations, the EEG provides an accurate picture of brain activity over a very short period of time.

The EEG is recorded during specific sensory stimulation, such as presentation of a flash of light or a tone. The component of the EEG related specifically to a significant stimulus is called a sensory-evoked potential or event-related potential. The EEG is recorded during repetitive natural stimulation, which activates sensory receptors and reflects the processing of the stimulus' physical characteristics [6].

3. FUNCTIONAL MRI AND VISUAL AREAS

3.1 Visualizing the brain using fMRI

Since patterns of current flow within the brain are so complex, a visualization of the cortical structure is essential for locating and analyzing source dipoles. The fMRI is ideal for brain imaging because it provides high-resolution reports of neural activity localized within a few millimeters of space and a few seconds of time. The image is created by a blood oxygen-level dependent signal, or BOLD signal, and is sufficient for the identification of stimulus-activated brain areas. Using this tool, we can identify positions of retinotopically organized visual areas and measure responses associated with contrast, color, and motion [3].

The magnetic resonance imaging hardware in the scan room consists of a magnet containing gradient coils and the RF coil to produce the magnetic field necessary for imaging. The control computer, located behind the RF shield, regulates the radio frequency and pulse and produces a sine wave of the desired frequency. The computer also controls the stimulus sequence that the subject views while laying inside the MRI magnet. The two stimuli used for our purposes were expanding rings and a rotating wedge, both made of an alternating black and white checkerboard pattern (Figure 3). These stimuli generated a wave of activity across the cortex, which allowed for the creation of a brain image [3].

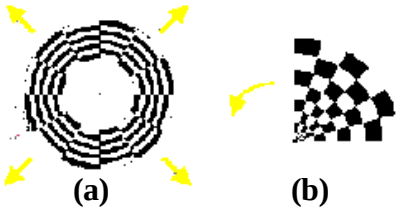

Figure 3: (a) Expanding ring and (b) rotating wedge stimuli used for fMRI data collection [1].

The two stimuli were designed to activate the visual cortex in different dimensions. The flickering checkerboard pattern of the stimuli caused an increase and decrease in neural response, sending a traveling wave of activity across the visual cortex. Expanding rings created phase-encoded visual responses and activated the cortex in the eccentricity dimension. The rotating wedge stimulus activated the angular dimension (Figure 4) [2].

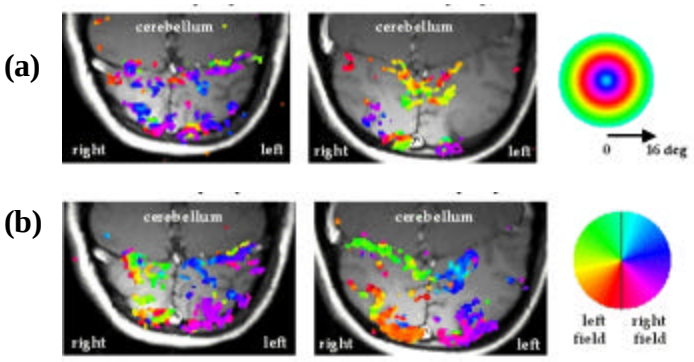

Figure 4: Superposition of phase data on fMRI inplane images showing cortical activation due to (a) expanding rings and (b) a rotating wedge stimuli [1].

3.2 Mapping visual areas using fMRI

After fMRI data has been collected and manipulated to produce a three-dimensional volume of the brain, the locations of visual areas can be identified. The visual cortex can be separated into these different regions, called visual areas, each with a complete retinotopic map. Visual area one, or V1, is the area of the brain that is also referred to as the visual cortex or striate cortex, and is the first area of the brain to receive information from the lateral geniculate nucleus, or LGN. The LGN, which is the primary location of retinal axon termination, and is an important part of the visual system since it is the principal subcortical region that processes visual information for perception [7].

Other cortical visual areas are V2 and V3, which augment analysis undertaken in V1. There are another two dozen distinct areas of cortex, each with its own retinotopic map. Along the parietal lobe we find area MT (V5), which seems specialized for analysis of motion, while the temporal lobe contains V4, which may be important for shape and color perception. The exact locations of these visual areas can be identified through fMRI analysis (Figure 5) [4].

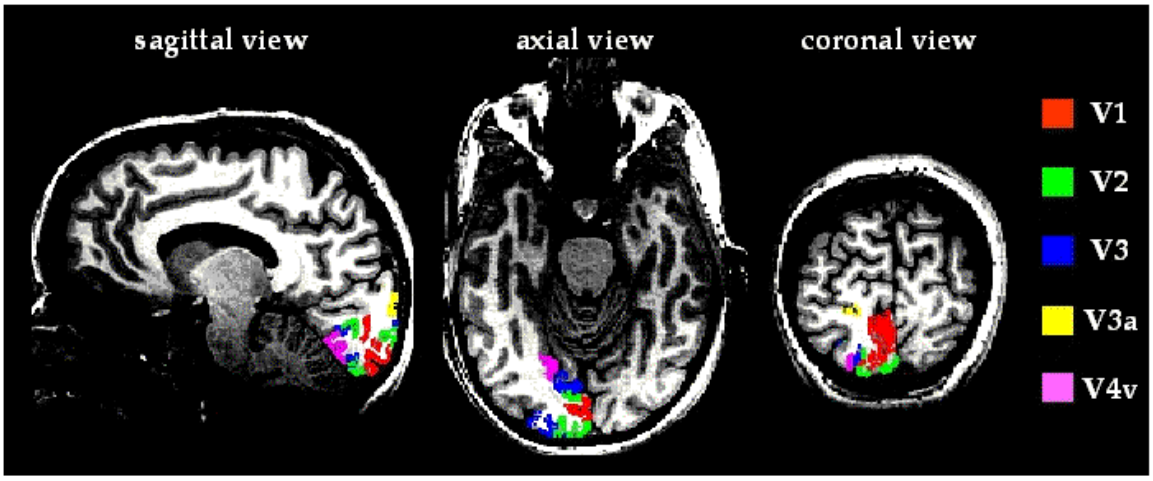

Figure 5: Locations of the visual areas V1, V2, V3, and V4 in the human brain [1].

4. EXPERIMENTAL DESIGN

4.1 Problem description

In order to test current scientific models of current flow within the head and to probe the visual pathways responsible for the flow of information from retina to visual cortex, we studied the variations in scalp potential generated in response to visual targets. We first used a metabolic technique, the fMRI, to provide us with a three-dimensional visualization of the subject's brain tissue. After pinpointing the source location within the visual cortex, we continued with further EEG study, which provided us with a scalp distribution pattern corresponding to source dipoles whose locations were already known.

For our electromagnetic research, we varied the contrast and flicker frequency of the stimulus in order to find characteristic response frequencies at multiples of the flicker frequency. By concatenating data collected from each block of trials, we produced a three-dimensional data cube defined by trial number, electrode number, and voltage amplitude. After Fourier analysis, Matlab and SigmaPlot were utilized to plot amplitude spectra, polar graphs, and contrast functions at different frequencies, which provided us with information about dominant visual pathways.

4.2 Equipment design

The setting for our experiments included a small laboratory with four computers: a MacIntosh to run the stimulus video in Matlab, a PC to collect behavioral data, a master to record psychophysical data in InstEP, and a slave to aid in system synchronization by presenting the stimulus video. An independent monitor behind a metal shield with a rectangular cutout at eye level showed the visual stimulus to the subject. The subject sat in a chair, head stationary in a chin rest, viewing the stimulus on the monitor through the hole in the metal shield. All electronic equipment was grounded and a heavy black

curtain drawn across the laboratory doorway kept the room in semi-darkness with only a small clip-on lamp providing illumination.

During experimentation, the subject wore an electrode cap with 28 electrodes positioned over specific places on the scalp, 2 separate electrodes stuck to the skin behind the ears, a single electrode stuck on the right temple, and a single electrode beneath the left eye (Figure 6). The two facial electrodes served to measure eye movements and the two electrodes behind the ears acted as reference points for measurements at scalp electrodes. The electrode cap was lined up precisely on the scalp and was held secure by straps snapped into place on the cap and tightly fastened to a chest strap. A large ribbon cable protruded from the top of the cap and was connected to an amplifier. Recorded potentials were amplified 10,000X, filtered at 0.01-100 Hz, and sampled at 300 Hz.

Figure 6: An array of 32 electrodes positioned on the scalp and labeled according to location.

Before every experiment, we replaced the amplifier battery, measured, adjusted and recorded electrode impedances. Electrode gel was inserted into each electrode with a blunt syringe until scalp electrode impedances fell below 5.0 μΩ and eye electrode impedances were no more than 10.0 μΩ. Once the electrode impedances were recorded, the subject's placement was precisely adjusted. Using a measuring tape and a level, we positioned the subject exactly 50.0 cm from the stimulus monitor with the subject's eyes lined up and level with the fixation point in the center of the monitor (Figure 7).

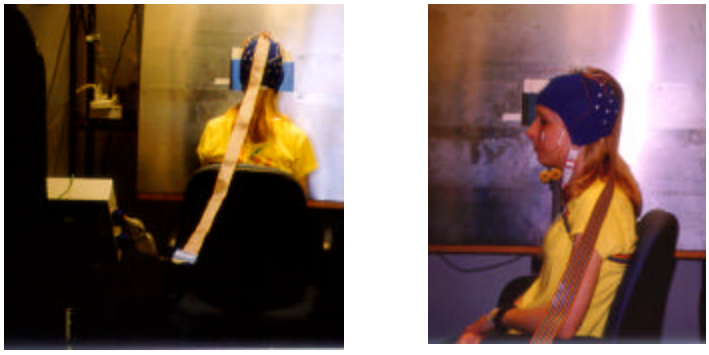

Figure 7: Subject wearing electrode cap and viewing stimulus through metal shield.

4.3 Stimulus design

For our experiment, the subject, holding a computer mouse, fixated on a small white square in the middle of the presentation monitor. The stimulus, shaped like a wedge at a fixed eccentricity, appeared and flickered at 7.5 Hz. At four or five seconds after presentation, the wedge changed color and the subject responded by clicking the appropriate mouse button: left button for a red color change, and right button for a green color change (Figure 8).

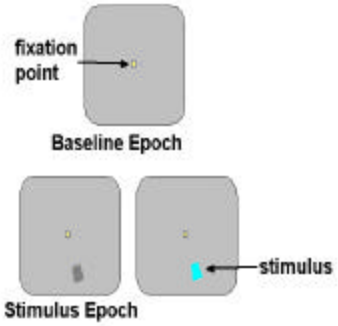

Figure 8: Stimulus flickered at 7.5 Hz with a color change at 4 and 5 seconds. Subject responded as soon as she detected color change.

The first block of trials contained a flickering wedge at a contrast of 6.5%, and each successive trial increased the wedge contrast to 12.5%, 25%, 50%, and 90% contrast. While viewing the stimulus on the computer monitor through the metal shield to block electrical interference, the subject wore the electrode cap connected to the amplifier to record scalp potentials. Along with the collecting of psychophysiological data, the mouse button clicks were recorded in order to assess behavioral performance.

5. DATA ANALYSIS

5.1 Psychophysical data

For each flicker frequency experiment, we collected and analyzed behavioral data to determine effective stimulus color tint values. When the stimulus wedge changed color randomly at four or five seconds after it appeared on the monitor, the color tint corresponded to parameters set in the Matlab stimulus video program. By recording each mouse button press in response to stimulus color change, we were able to compare the collected right and left button presses for accuracy. Three different tint values were specified in the Matlab program, and were set to produce behavioral results where performance decreased as tint level decreased.

In order to make sure that the color change detection task was set at a proper difficulty level, we plotted the subject's performance at each tint level. While the task had to be difficult enough to force the subject to concentrate and focus her attention, it also had to be easy enough so that she was not overly frustrated when determining the correct color change. We manipulated tint values within the Matlab program to obtain a sensible

performance curve where we were confident that the subject was comfortable attending to the task (Figure 9).

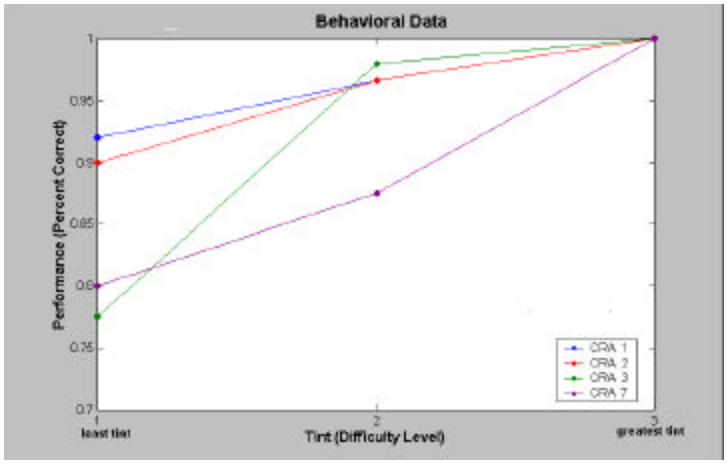

Figure 9: Behavioral data shows performance decreases as tint values become more difficult to perceive.

5.2 Psychophysiological data

Analysis of the EEG recordings with Fourier analysis proceeded with Matlab graphs of amplitude spectra and polar plots. By separating frequency components of the recorded scalp potential, the amplitude spectra graphs plotted signal amplitude in microvolts versus signal frequency in Hertz at each individual electrode. Frequency spikes were analyzed to give insight into the characteristics of the collected response. The experiment was entitled CRA6, since it was the sixth test in a series of contrast response analysis studies. The experiment utilized a flicker frequency of 7.5 Hz and frequency spikes were recorded at approximately 10 Hz and 15 Hz. When the contrast was set at a maximum value of 90%, the amplitude at 15 Hz was 1.2759 μV; at 50% contrast, the amplitude was 0.8902 μV (Figure 10).

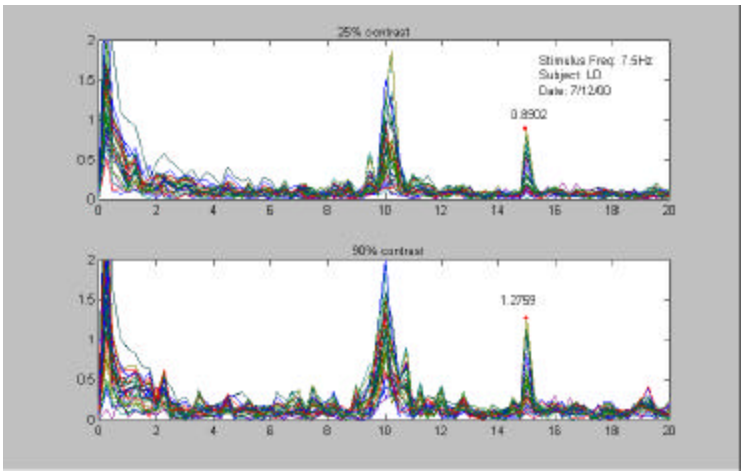

Figure 10: Amplitude spectra for experiment CRA6 at (a) 50% and (b) 90% contrast.

While the ten Hertz frequency component is a characteristic brain wave called alpha that is present in all of the subject's EEG recordings, the 15 Hertz component is more interesting: it provides information about the frequency response of neural cells in response to the stimulus. These preliminary findings show that Fourier analysis produces amplitude spectra containing a response at twice the fundamental flicker frequency. A polar plot of each individual electrode's amplitude and phase at 15Hz shows that they are roughly in phase and that the maximum amplitude is recorded at electrode PO4 (Figure 11).

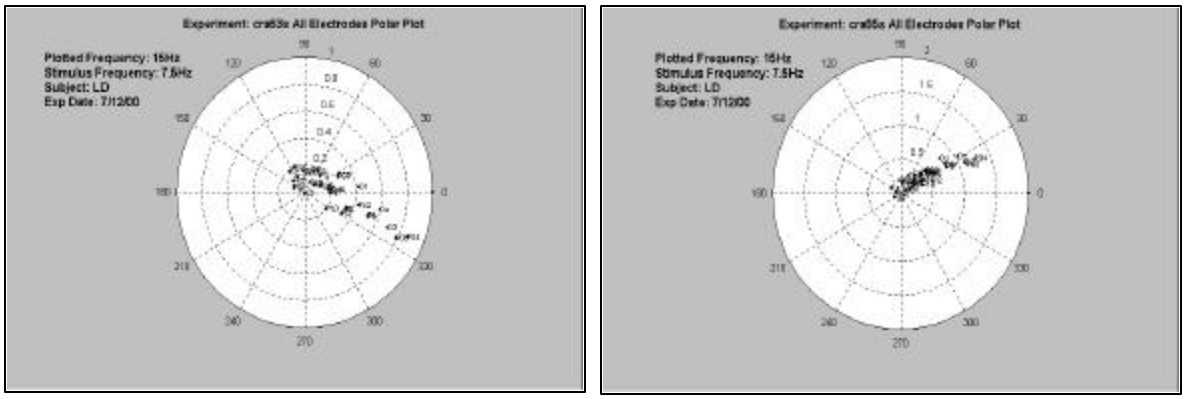

(a) **(b)**

Figure 11: Polar plots of amplitude and phase at each electrode at 15 Hz for a flicker frequency of 7.5 Hz at (a) 50% and (b) 90% contrast.

Further analysis of the data was carried out by plotting the responses at each contrast value to obtain an approximation of the subject's contrast response function. Since the subject's maximum response amplitude was recorded at electrode PO4, we calculated the signal amplitude at PO4 at 7.5 Hz (the fundamental flicker frequency) and at 15 Hz (twice the fundamental flicker frequency) at all five contrast values. Using

SigmaPlot, we compared our experimental data with the best-fit contrast response function (Figure 12).

Contrast Response Graph

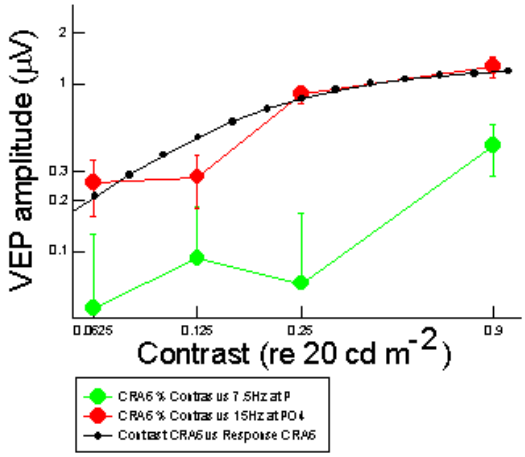

Figure 12: Signal amplitude versus percent contrast at 7.5 Hz (green) and 15Hz (red) for electrode PO4 compared with the best-fit contrast response function curve (black).

6. DISCUSSION AND CONCLUSIONS

6.1 Source analysis

By combining our metabolic fMRI data and electromagnetic EEG recordings, we tested the widely used three-shell conductivity model of the head and followed a different approach to the source analysis problem. Instead of using complex scalp potential patterns to pinpoint the current source within the brain, we first used fMRI data to locate the origin of our signal. Through this method, we hoped to reveal flaws in the broadly accepted three-shell model, where the human head is modeled as a volume conductor having three concentric shells of uniform conductivity.

When the three-shell model is used for source analysis, the scalp potential distribution depends on both the locations and orientations of dipoles within the brain and the thicknesses and conductivities of the shells. The outermost shell is the scalp; the middle shell is skull; and the innermost shell is the entire brain and surrounding cerebrospinal fluid. Each shell has a different conductivity and forms a boundary which distorts current flowing within.

Although the three-shell model has been used by many researchers studying the problem of source analysis, we recognized several flaws that could cause misleading experimental results. Although this model is convenient, it oversimplifies the complex structure of a human head. For example, in this model, brain and cerebrospinal fluid have one constant conductivity value and are one homogeneous shell. Intuition suggests that it

is inaccurate to assume that materials with such widely varying conductivity values can be considered one homogeneous shell (Figure 13).

Material	Conductivity (S/cm)	Resistivity (ohm*cm)
Copper	5.0×10^{6}	2.0×10^{-6}
Seawater	5.0×10^{-2}	2.0×10^{1}
CSF	1.6×10^{-2}	6.4×10^{1}
Cortex (5 Hz)	2.9×10^{-3}	3.5×10^{2}
White matter (avg)	1.5×10^{-3}	6.5×10^{2}
Wet skull (low frequency, avg)	5.0×10^{-5}	2.0×10^{4}
Pure water	5.0×10^{-8}	2.0×10^{7}

Figure 13: Conductivity values for the three-shell model where outermost shell is scalp, middle shell is skull, and innermost layer is entire brain and surrounding fluid.

Experimental evidence also reveals flaws in this simplified model. The three-shell approximation predicts that a stimulus presented on one side of the vertical meridian should activate a contralateral area in the brain. Therefore, if a stimulus flickers on the right, increased response amplitude should be recorded on the left side of the scalp. Conversely, a stimulus located on the left side should result in a larger response in right electrodes.

The data collected from our repeated experiments disagree with the predictions made by the three-shell model. Our data did not show the expected contralateral increase in potential amplitude. Instead, certain electrodes always recorded greater voltages no matter where the stimulus was positioned. When the stimulus was rotated around the fixation point at a constant eccentricity and flickering at 7.5 Hz, the same area of visual cortex was activated, and the same 15 Hz frequency was detected at electrodes at all positions on the scalp (Figure 14). In addition, the response did not vary according to whether the stimulus was on the right or left side of the vertical meridian; maximum amplitude always occurred on the subject's right hemisphere. The data we have collected invalidates the three-shell model, and instead supports a more complex model of inhomogeneous conductivity.

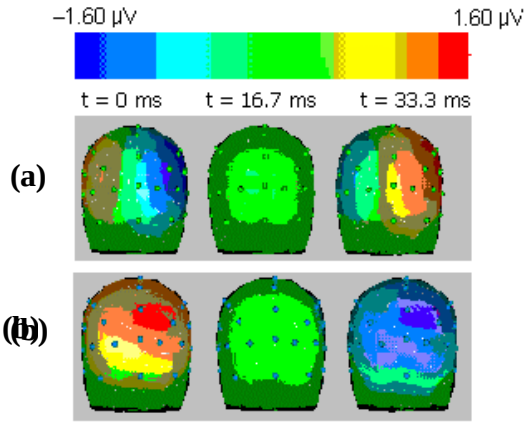

Figure 14: The (a) predicted scalp distribution for V1/V2 dipole source does not correspond with the (b) experimentally observed scalp

6.2 Cellular interrogation

By recording and analyzing the sensory-evoked potentials associated with our carefully designed stimulus, we were able to deepen our understanding of cortical organization and the visual information processing process. We used fMRI brain volume data for source analysis, which allowed us to model a dipole source responsible for the EEG spatial pattern. Taking this a step further, we also identified the pathway responsible for transferring the information processed by the retina to the identified visual area.

We already have evidence of two main visual pathways: the magnocellular or M pathway and the parvocellular or P pathway. The existence of two separate pathways suggests that parallel processing occurs in the visual system where retinal neurons project information to different cells in the central nervous system. It is believed that the M pathway handles the initial analysis of visual image movement, while the P pathway deals with the examination of fine structure and color vision. The inputs of the cells involved in the M and P pathways are segregated anatomically into different cellular levels [7].

In order to avoid using the three-shell model, we did not use the conventional method of analyzing EEG data to locate the source of activity. Instead, we began our investigation into the location of the dipole source by using fMRI data to get a good visualization of the organization of the visual cortex. To conduct our fMRI data collection, we visited Stanford Vision and Imaging Science and Technology Group run by Dr. Brain Wandell at Stanford University. Using the MRI imager and related computer programs, such as mrLoadRet and mrGray, we were able to produce a three-dimensional volume of our subject's brain.

After fMRI data collection, we used computer simulators to unfold the cerebral cortex, since the cortical surface is compressed inside the skull. Before unfolding into a single image, measurements were integrated from several different images by segmenting the gray matter in a series of image planes. Then we superimposed the fMRI responses to our different stimuli on the unfolded brain to visualize the patterns of neural activity in the visual cortex. Because the stimuli generate traveling waves that reverse direction at visual area boundaries, after we created our two-dimensional maps, we were able to pinpoint the locations of our sought-after visual areas, and therefore, our source dipoles [3].

Since we know where the visual areas are located within the physical structure of the brain, we designed our EEG stimulus to activate those specific areas. Our graph plotting the contrast response function, which shows how the scalp potential amplitude varies with contrast at a specified frequency, allowed us to determine which visual areas were activated and which pathway was responsible (Figure 9).

The contrast response graph showed that at 15 Hz, the response saturates at 25% contrast, suggesting that our data can be modeled by a hyperbolic saturation curve, which is described by the following equation:

$$R = R_{max} * \frac{C^n}{C^n + C_{1/2}^n}$$

This curve relating the response of a cell, R, and the contrast, C^n, of its preferred sine wave grating predicts a linear increase in signal amplitude at low contrast values, and a level amplitude at high contrast values, which matches our experimental data. The parameters R_{max}, n, and $C^n_{1/2}$ characterize respectively the maximum response, the slope of the rising part of the curve, and the gain. Therefore, $C^n_{1/2}$ is the semi-saturation constant and the value of n indicates whether the magnocellular or parvocellular pathway is dominant [5].

The contrast function that we derived from our experimental data has a best-fit hyperbolic saturation contrast response function where the variables R_{max} and n corresponded to values of 1.9 μV, and 2.2, respectively. This result implicates the processing of information via the magnocellular pathway. Also, the MRI map of the human brain has proved that our specific flickering stimulus activated the visual areas V1 and V2. By combining these two results, we obtained our sought-after result: the activation of V1 and V2 involves a magnocellular response. Thus, we have experimentally validated the suggestion that the M pathway is specialized for the analysis of object motion.

6.3 Further Research

Now that we have tested the three-shell model and shown its shortcomings, the next step in tracing cellular pathways is to propose a new model that can properly represent the human head and the flow of current within. Further research involves investigation into the inhomogeneous model and how it can help us analyze the dipole current sources that generate measurable scalp potentials.

7. ACKNOWLEDGMENTS

I would like to thank Dr. Nader Engheta, Dr. Edward N. Pugh, Claire Daniele, and Lauren Daniele for their guidance and encouragement. Because of their assistance and enthusiasm throughout this project, I gained valuable research experience and strengthened my knowledge of basic principles underlying the seemingly diverse areas of psychology, electrical engineering, and neuroscience. I also appreciate the National Science Foundation's commitment to supporting undergraduate research in sensor technologies at the University of Pennsylvania.

8. REFERENCES

1. Baseler, Heidi, "Retinotopy Analysis and Visual Area Identification" Stanford Vision and Imaging Science and Technology, 1999. http://white.stanford.edu/~heeger/labmanual/retinotopy.html (2000, July 23).

2. Bear, Mark F., Barry W. Connors and Michael A. Paradiso, eds. Neuroscience: Exploring the Brain. Baltimore: Williams & Wilkins, 1996. 240-638.
3. Engel, Stephen A., Gary H. Glover and Brian A. Wandell, "Retinotopic Organization in Human Visual Cortex and the Spatial Precision of Functional MRI", *Cerebral Cortex*, 7 (1997) 181-192.
4. Kandel, Eric R. "Perception of Motion, Depth, and Form." Principles of Neural Science. Comp. and Ed. Eric R. Kandel, James H. Schwartz, and Thomas M. Jessell. New York: Elsevier, 1991. 441-466.
5. Lennie, Peter, "Single Units and Visual Cortical Organization", *Perception*, 27 (1998) 889-935.
6. Martin, John H. "The Collective Electrical Behavior of Cortical Neurons: The Electroencephalogram and the Mechanisms of Epilepsy." Principles of Neural Science. Comp. and Ed. Eric R. Kandel, James H. Schwartz, and Thomas M. Jessell. New York: Elsevier, 1991. 777-790.
7. Mason, Carol and Eric R. Kandel. "Central Visual Pathways." Principles of Neural Science. Comp. and Ed. Eric R. Kandel, James H. Schwartz, and Thomas M. Jessell. New York: Elsevier, 1991. 420-439.